Quantifying the Mechanisms of Site-Specific Ion Exchange at an Inhomogeneously Charged Surface: Case of Cs+/K+ on Hydrated Muscovite Mica

Narasimhan Loganathan, Andrey G. Kalinichev

Quantifying the mechanisms of site-specific ion exchange at an inhomogeneously charged surface: Case of Cs^+/K^+ on hydrated muscovite mica

Narasimhan Loganathan[1,#], Andrey G. Kalinichev[1,*]

[1] Laboratoire SUBATECH (UMR-6457), Ecole des Mines de Nantes, 44307, Nantes, France

[#] Present address: Department of Chemistry, Michigan State University, East Lansing, MI 48824, USA

* Corresponding author: mail: kalinich@subatech.in2p3.fr

Abstract

Adsorption and mobility of radioactive Cs^+ isotopes in soil are among the most important factors affecting the long term environmental footprint of nuclear accidents such as Chernobyl (1986) and Fukushima Daiichi (2011). In particular, Cs^+ ions can be retained through their exchange with K^+ naturally present in muscovite mica, one of the common soil mineral components. ClayFF force field allowed us to realistically represent local inhomogeneities of the structure, composition, and charge on the muscovite (001) surface, and to identify three structurally different types of adsorption sites. We performed molecular dynamics simulations of Cs^+ and K^+ adsorption at the hydrated muscovite surface and used quasi-one-dimensional site-specific potential of mean force calculations to quantify the energetics of ion exchange in this system for each individual site and for the entire muscovite surface on average. Irrespective of the type of adsorption site, both K^+ and Cs^+ cations are preferably adsorbed on the basal (001) muscovite surface at the centers of ditrigonal cavities as inner sphere surface complexes. The free energy difference between the most favorable and the least favorable surface sites for Cs^+/K^+ ion exchange amounts to 11.7 kJ/mol, with the most favorable sites occupying half of the surface, the least favorable type – 1/6 of the surface, and the rest exhibiting an intermediate adsorption and ion exchange capacity. The simulation results are compared with available thermodynamic estimates based on recent X-ray reflectivity measurements.

Introduction

Sorption of ions at mineral surfaces often controls their distribution in both natural and technological settings.[1-5] The adsorption and retention properties of toxic elements by soil components, such as clay minerals, determine their transport in near-surface and sub-surface environments. These properties are strongly affected by two important factors: (*i*) structure and composition of the mineral substrate[5,6] and (*ii*) near-surface solution structure which is different from that of bulk aqueous environments.[7-9] The structure and mobility of aqueous species at clay mineral interfaces have been extensively investigated in recent years by various experimental[10-16] and computational molecular modelling[17-24] techniques. These works have provided important molecular scale information on such properties as ion adsorption, surface hydration structure, orientational and diffusional dynamics for several monovalent and divalent cations and H_2O molecules. However, there is often a considerable discrepancy between the properties predicted using thermodynamic modeling and those observed experimentally.[25,26] For instance, Bourg and Sposito[27] have identified Na^+ adsorption environments at smectitic surface contrasting those predicted by the triple layer model theory. The study also indicated that properties such as electroosmosis arising from long range electrostatic interactions could not be properly predicted by the thermodynamic surface speciation models. One of the main reasons for such descrepancies is the simplification of the conventional surface models used to explain the adsorption phenomena. The ion adsorption strength and distribution coefficient at clay surfaces is usually described by a single surface-specific constant. For example, X-ray reflectivity studies[28] use a single surface-averaged value for the free energy of adsorption (ΔG) for Rb^+ and Sr^{2+} ions at the muscovite surface. Similarly, simulation studies provide a single value for diffusion coefficients of hydrated ions for the entire basal surface.[7,9,21-24] The dependence of these properties on the

existence of different types of adsorption sites at the clay surfaces is not usually taken into account and is difficult to determine experimentally.[16,25] However, with recent advances in computational molecular modeling of such systems, a detailed site-specific information about the structure, dynamics, and energetics of interfacial aqueous species can now be obtained and quantified on a fundamental atomistic scale.

The interfacial properties of muscovite mica, a phyllosilicate mineral which is abundantly present in soils and sediments, have been widely investigated.[9-15,17-20] The high structural charge of muscovite is responsible for the adsorption of hydrated cations at its surface through electrostatic forces.[29] Contrary to chemisorption, where experiments and thermodynamic models can predict the active site interactions with specific ligands,[30] physisorption is often difficult to examine because of its much weaker character and the absence of new covalent bonds formed. For instance, ions can be adsorbed both as inner sphere surface complexes (IS) or outer sphere surface complexes (OS) and different thermodynamic models are used to describe the interfacial properties.[31-33] Although the most advanced experimental techniques can now probe the energetic and structural distribution of such surface complexes in a surface-averaged way, it is still difficult to obtain more detailed data about the adsorption at various individual surface sites and their corresponding energetic contributions.[34]

At the same time, muscovite mica is a significant substrate surface in geo- and environmental chemistry because of its high cation exchange capacity.[32-41] Its structurally present K^+ ions can be easily exchanged for other cations at the hydrated basal surface of muscovite. Cs^+ ion is one of the most important cations to consider in this context, because its various isotopes represent significant components of radioactive waste.[25,37-40] The isotope ^{137}Cs has been introduced in the environment by weapons testing and nuclear accidents, other quite common

radioisotopes are ^{134}Cs and ^{135}Cs, the latter of which is extremely long lived. Because of its high aqueous solubility and chemical similarity to K^+, Cs^+ can be easily assimilated by living organisms, and its bioavailability is essentially controlled by the adsorption and retention properties of the solid phases in the environment. The need for in depth quantitative molecular scale understanding of the Cs^+/K^+ exchange at the muscovite surface has been further recognized in the aftermath of the Fukushima Daiichi nuclear accident of 2011.[41-46]

The main objective of the present study is to develop a quantitative approach to assess the ion adsorption and exchange capacity of individual adsorption sites on heterogeneously charged substrates, such as basal surfaces of clay minerals, and to evaluate the effects of site specificity on the adsorption and exchange properties of K^+ and Cs^+ ions at the muscovite surface using molecular dynamics (MD) simulations and free energy calculations. We use MD simulations and potential of mean force (PMF) calculations to evaluate not only the adsorption free energy of the ions as function of their distance from the surface,[7,47] but adapt this technique to probe specific adsorption sites on the surface. The energetic contributions of each structurally different adsorption site for K^+ and Cs^+ are thus evaluated. A complete description of cation exchange reaction equilibria is represented and the corresponding thermodynamics parameters are discussed in detail and compared with available experimental data.

Molecular Models and Simulation Details

Muscovite mica is a 2:1 layered aluminosilicate mineral with the crystallographic unit cell formula $KAl_2(Si_3Al)O_{10}(OH)_2$. Its so-called T-O-T structure formed by a sheet of $AlO_4(OH)_2$ octahedra sandwiched between two sheets of SiO_4 tetrahedra, which are arranged within the sheet

into a lattice of six-member rings having ditrigonal symmetry. These aluminosilicate T-O-T layers are stacked along the direction of the surface normal. There are several sources of crystallographic parameters for muscovite mica that are all well consistent with each other.[48] The AFM data[49] were selected here as a primary source of the initial structural parameters for our muscovite surface models for two reasons: (*i*) they refer specifically to the experimentally probed muscovite surface – the principal focus our our investigation; (*ii*) multiple previous studies have already demonstrated that this muscovite model reproduces well the experimental crystallographic cell parameters of bulk muscovite and yields highly dependable results for muscovite surfaces.[9,45,50-53] In the muscovite model structure, 1/4 of all Si atoms in the tetrahedral sheets are isomorphically substituted by Al resulting in a net negative structural charge of muscovite, which is compensated by the presence of the interlayer K^+ cations occupying every ditrigonal ring in the structure. The simulation supercell was constructed out of 6×3 unit cells resulting in the lateral dimensions of $L_x = 31.21$ Å and $L_y = 27.07$ Å for our model. In contrast to earlier simulations,[50-54] this surface is sufficiently large to permit a random arrangement of isomorphic Al/Si substitutions within each tetrahedral sheet, yielding a realistically disordered distribution of the structural charge. This arrangement avoids any regular long-range pattern of Al/Si substitution and is also in accordance with the Lowenstein's rule (forbids Al-O-Al linkages).[48] A special care was taken to eliminate any presence of structural charge gradient at the muscovite surface during this process of creating a macroscopically uniform but locally inhomogeneous distribution of structural charge. As a result, each tetrahedral sheet consisted of ditrigonal rings of either Si_4Al_2 or Si_5Al composition in equal proportions randomly distributed within the structure and yielding 3 different adsorption sites for the charge compensating cations which are labelled as follows: **1a** - two Al tetrahedra are symmetrically placed across each other in the ditrigonal ring and separated by the presence of two Si tetrahedra

in the same ring; **1b** – two Al tetrahedra asymmetrically separated in the ring by one and three Si tetrahedra from each side, making them in closer proximity to each other than in the symmetric case; **1c** – a ditrigonal ring containing only one Al substitution (see Figure 1). All interlayer K^+ ions are located at the centers of ditrigonal rings between two adjacent T-O-T layers and are strongly coordinated to the basal surface bridging oxygen atoms.

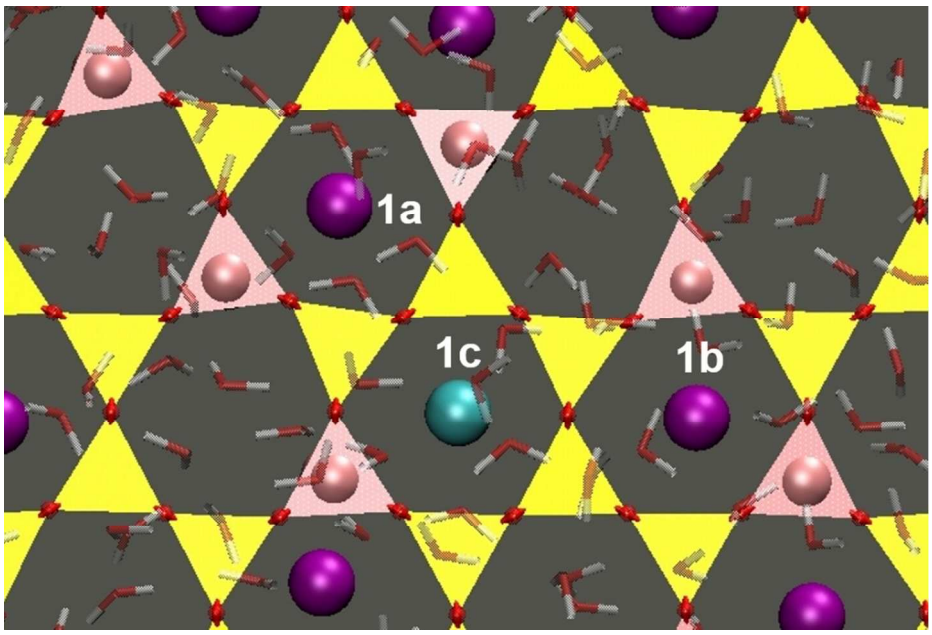

Figure 1. Schematic representation of the hydrated basal muscovite surface illustrating 3 structurally different adsorption sites. Al – Pink; Si – yellow; O – red, H – gray; K^+ – purple, Cs^+- cyan. (Only one tetrahedral sheet is shown for clarity).

The model muscovite-water interface was built by first cleaving the bulk crystal structure along the (001) plane at the middle of the interlayer space. After cleavage, half of the interlayer K^+ ions located at the ditrigonal cavities were randomly retained by each of the two surfaces

created. Empty space was added on top of the surface, filled with water molecules to ensure at least ~16 molecular layers of H_2O at each surface at the density of liquid water under ambient conditions, and the resulting simulation supercell consisted of 2 muscovite T-O-T layers with a total thickness of ~20 Å and the aqueous layer ~96 Å thick separating two surfaces of the cleaved crystal. The large thickness of the aqueous layer effectively eliminated any effect of one hydrated surface over another when the periodic boundary conditions were applied during the simulations and hence creating two statistically independent and statistically equivalent interfaces of a thickness comparable to those observed in X-ray reflectivity measurements.[14,15,29,34]

Only one K^+ ion was replaced by Cs^+ ion at each surface. Initially, all the cations were pulled up to 10 Å away from the respective surfaces which allowed them to arbitrarily settle on their preferred adsorption sites during the preliminary equilibration MD run. All MD simulations were performed in the canonical *NVT* ensemble at 300 K using the LAMMPS simulation package.[55] All interatomic interactions were calculated using the ClayFF set of interaction potentials, which includes the SPC model for water molecules.[56] A cutoff distance of 10 Å was applied for the calculation of short range non-electrostatic interactions, while the standard Ewald summation technique was used to treat the long range electrostatic interactions between the atomic charges. A time step of 1 fs was used to integrate the equations of motion. The system was initially equilibrated for 1 ns with a subsequent equilibrium MD run of 1 ns with atomic coordinates recorded every 10 fs for the calculation of adsorption and structural properties.

It is important to note that all atoms of the muscovite structure were allowed to fully relax in all three dimensions during the pre-equilibration stage of MD simulations. They were not fixed during the equilibrium MD runs either. Thus, the muscovite surface remained atomistically corrugated on a small scale due to occasional small rotations of the tetrahedra. Since there are no

explicit bonds between Si and O atoms in the ClayFF model,[56] the tetrahedra are held together together by solely electrostatic and van-der-Waals terms of the interatomic potentials.

Potential of mean force calculations

The adsorption free energy profiles of K^+ and Cs^+ ions as a function of their distance from the muscovite surface at thermodynamic equilibrium were determined using potential of mean force (PMF) calculations. At first, the most preferred adsorption sites for both K^+ and Cs^+ ions at the muscovite surface were identified in preliminary unconstrained MD simulations from time-averaged atomic density profiles along the direction normal to the surface and planar atomic density distributions in molecular planes parallel to the surface. Unlike smectite clay substrates characterized by lower charge density, where two structurally different adsorption sites were identified on the tetrahedral surface (at the center of ditrigonal rings and on top of Si tetrahedra),[23,24] the muscovite surface with a much higher charge density allows for only one type of sites, the centers of the rings, for both K^+ and Cs^+. However, the sites still differ within this type by their local charge distributions due to the different mutual positions of Si and Al tetrahedra in the ring (Fig. 1).

A representative equilibrium structure from the preliminary simulations was then taken as a starting point for the PMF calculations, which were performed with the NAMD simulation package[57] using the collective variable analysis procedure[58] embedded in the code. All other parameters and conditions of the constrained MD simulations were the same as for the unconstrained MD runs described in the previous section. For the PMF calculation, a single K^+/Cs^+ ion was gradually pulled normal to the muscovite surface from its equilibrated position and constrained at certain distance using a harmonic biasing potential. A force constant of

50 kcal/mol Å^2 was used in all simulations and the distances were probed in the range from 1.0 Å (K^+) and 1.5 Å (Cs^+) up to 10 Å with a step of 0.1 Å until 6 Å and 0.2 Å thereafter. All other atoms, including the structural atoms of the mica surface, remaining interfacial cations, and water molecules were free to move during the simulation and were not fixed at their equilibrium positions in contrast to previous Monte Carlo ion-muscovite PMF calculations.[54,59] For each distance *z*, the system was equilibrated in an MD run of 1 ns and the data were collected from the additional 1 ns simulation run. After obtaining the biased (constrained) distributions for all distances, the results of all simulations were combined using the weighted histogram analysis method,[60] and the effect of the biasing potentials was removed to extract the unconstrained free energy profiles.[61]

However, it is impossible to obtain a site-specific adsorption free energy profile by constraining only the distance from the surface in MD simulations because the cations remain free to move laterally along (*x*-*y*) directions parallel to the surface and away from the initial surface site, thus distorting the site-specific nature of the profile. We have overcome this difficulty by applying additional harmonic boundary and wall restraints acting laterally. By having these additional weak restraints (force constants of 0.3 kcal/mol Å^2 and 0.4 kcal/mol Å^2 were used for boundary and wall restraints, respectively), we were able to restrict the lateral movements of the cation by holding it within certain limits along the normal above the selected adsorption site. By selecting very low values of the force constant for these supplementary restraints applied in the directions orthogonal to the much stronger primary restraint we ensured that the total effect of the restraints lead to a quasi-one-dimensional free energy profile along the direction normal to the surface and specific to each individual adsorption site. In other words, the K^+/Cs^+ ions were allowed to probe a very narrow cylindrical space with a diameter of 0.2 Å above each selected adsorption site at all distances from the muscovite surface (see Figure 2).

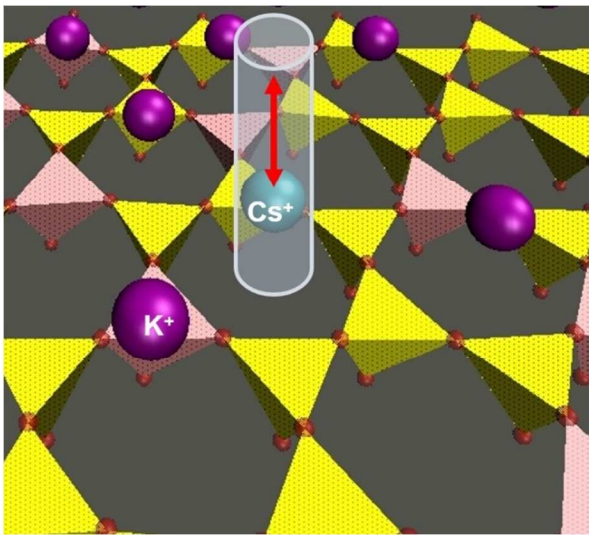

Figure 2. A schematic view of the tetrahedral muscovite surface indicating the metal ions (K^+/Cs^+) probing a narrow cylindrical space normal to the muscovite surface above a specific adsorption site. The origin of the vector normal to the surface is defined by the center of mass of 6 surface bridging oxygen atoms of the ditrigonal ring forming the adsorption site.

Results and Discussion

The PMF calculations were performed for all three identified adsorption sites (Fig. 1) in order to provide quantitative information on their site-specific adsorption strength and exchange mechanisms. In all three cases, the distance constraints were applied between the adsorbed cation (K^+/Cs^+) and the center of mass of 6 oxygen atoms of each adsorption site.

Adsorption of K^+ on hydrated muscovite

Figure 3 presents the calculated PMF profiles of K^+ ions at the hydrated muscovite surface for all three adsorption sites identified in Fig.1. Irrespective of the adsorption site, the minimum in the PMF profiles is at ~1.6 Å from the muscovite surface, which is consistent with the previous simulations[50,54] and X-ray reflectivity measurements,[34] and is obviously mostly dictated by the closest contact distance between the K^+ ion and six bridging oxygens forming the ditrigonal ring of the adsorption site. However, despite having similar equilibrium adsorption distances, the free energy minima are significantly different between these three sites. The most stable adsorption state for K^+ at the hydrated muscovite surface is at site **1a** (Fig.1) with the energy minimum of -41.8 kJ/mol, while the sites **1b** and **1c** are characterized by the energy minima of -31.4 kJ/mol and -25.1 kJ/mol, respectively. (It should be noted that the energy value at z = 10.0 Å, assumed to be large enough distance from the surface to represent a completely desorbed cation, was selected here as a common reference for comparison between different PMF profiles.)

All three sites clearly represent inner sphere (IS) surface adsorption complexes. At the same time, a very broad and much weaker outer sphere (OS) surface complex is evidenced at distances around 4-5 Å from the surface for all adsorption sites with the energy differences of -36 kJ/mol (**1a**), -28 kJ/mol (**1b**) and -22 kJ/mol (**1c**) relative to their corresponding IS complexes. In addition, an almost negligibly weak OS surface complex is observed for the **1a** and **1b** sites (both having two Al/Si substitutions in the ring) at distances around 6–8 Å. This confirms the notion that the IS adsorption complex is the most stable state for K^+ ion at the hydrated muscovite surface and is in agreement with experimental data[62] and previous simulations.[50,54] It is also worth noting that a characteristic change in the slope of the PMF is seen at distances around 3.2 Å for all three adsorption sites, which is most probably a signature of a substantial structural

rearrangement of the first molecular layer of interfacial water molecules when the ion is detached from the surface site to distances larger than the size of the H_2O molecule.

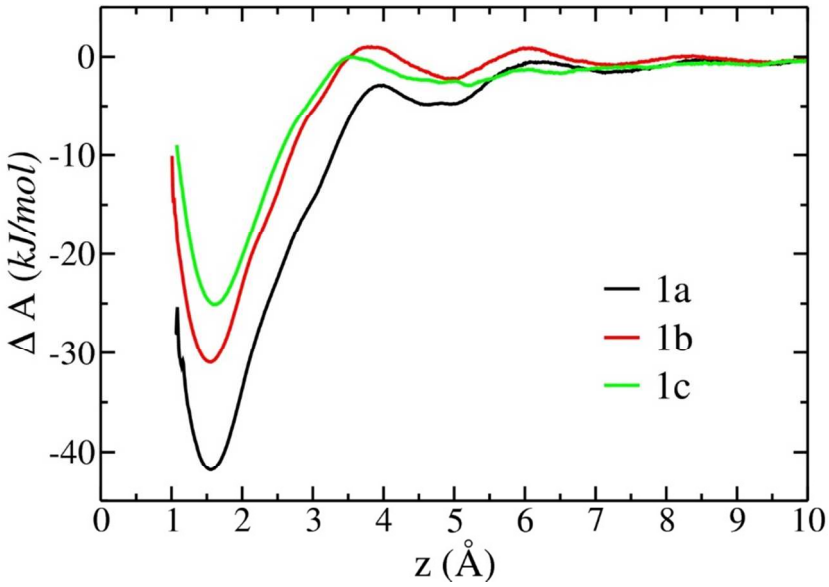

Figure 3. Adsorption free energy profiles for K^+ ions as a function of distance for three different adsorption sites on the muscovite basal surface. The adsorption sites **1a**, **1b**, and **1c** are defined in Fig.1.

Adsorption of Cs^+ on hydrated muscovite

The calculated adsorption free energy profiles for Cs^+ ion on the hydrated muscovite surface for all three different adsorption sites are shown in Figure 4. Like in the case of K^+, the energy minimum is at distances around 2.0 Å from the surface for all three adsorption sites and is consistent with experimental data.[34,62]

Although the energy minima for sites **1b** and **1c** are within 1 kJ/mol of each other and are both around -25 kJ/mol, the site **1a** again represents the most stable adsorption state with the

energy minimum around -30 kJ/mol. However, all of them represent IS adsorption complexes. A very broad and weak OS adsorption complex is evidenced by the presence of the energy minima around -2.5 kJ/mol in the range of 4-6 Å from the surface for all three adsorption sites. However, the energy barrier between the IS and OS surface complexes is very high with the range between -20 to -25 kJ/mol. Such an outer sphere surface complexation is possible only when there is high concentration of Cs^+ ions in the interfacial aqueous solutions.

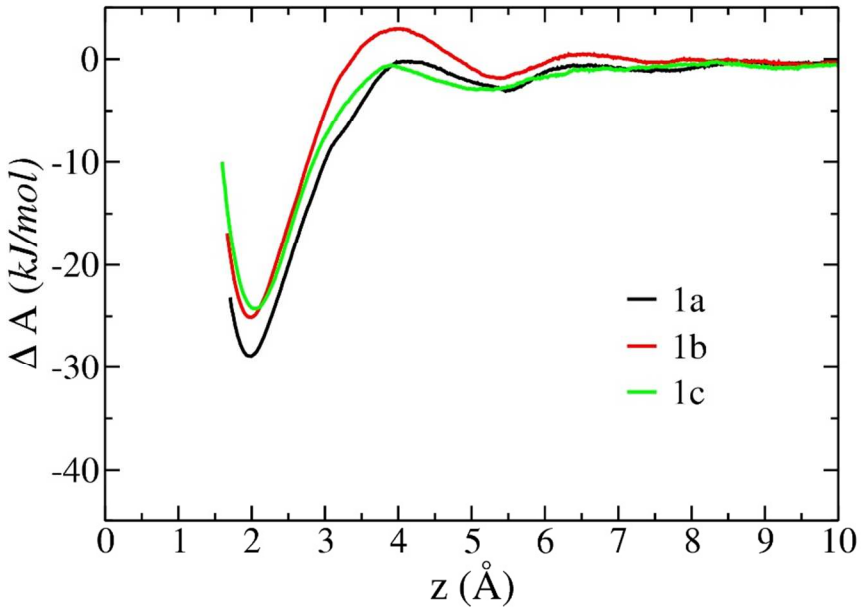

Figure 4. Adsorption free energy profiles for Cs^+ ions as a function of distance for three different adsorption sites on the muscovite basal surface. The adsorption sites **1a**, **1b**, and **1c** are defined in Fig.1.

Local surface charge inhomogeneity and its effect on K^+/Cs^+ adsorption

Irrespective of the adsorption site and the nature of the cation, IS adsorption represents the most stable surface complex at the muscovite-water interface. Such an adsorption structure is

dictated primarily by the presence of high structural charge at the muscovite surface, strong electrostatic attraction of the cations, and hence presents a very high energy barrier for the formation of an OS surface complex or a complete desorption. Also, regardless of the cationic nature, the strength of the stable adsorption sites is ordered in a sequence of **1a** > **1b** > **1c**, which could be partially attributed to the nature of interaction potentials used in the simulation. In the ClayFF parameterization, tetrahedrally coordinated Al atoms (at) bear a partial charge of 1.575|*e*|, compared to 2.1|*e*| for tetrahedrally coordinated Si atoms (st).[56] In addition, the bridging oxygen atoms around substituted Al tetrahedra (O_{bts}) have a charge of -1.16875|*e*|, which is ~11% more negative than the charge of ordinary bridging oxygen atoms (O_b) of Si tetrahedral, i.e., -1.05|*e*|, while the sizes of all oxygen atoms are assumed the same in this model.[56] Hence, there exist local charge inhomogeneities individually characterizing each adsorption site. The sites **1a** and **1b** are slightly more attractive for cations (4 - O_{bts} and 2 - O_b) compared to the site **1c** (2 - O_{bts} and 4 - O_b), which explains, of course, why the latter site shows a less negative energy minimum than the other two. Interestingly, in the case of a symmetric site **1a** (Fig.1), the increase of local charge density is more evenly distributed over the entire ditrigonal cavity, while for the site **1b** the same amount of extra negative charge is asymmetrically distributed over one half of the ditrigonal cavity. As it turns out, even such relatively minor local charge inhomogeneities can noticeably affect the short range cation-surface electrostatic interactions, and hence sites **1a** exhibit stronger and more stable coordination with the cations than sites **1b**.

Thermodynamics of Cs^+/K^+ exchange

The energetics of Cs^+/K^+ exchange reactions can be evaluated by using the individual site specific adsorption energies obtained through the PMF calculations and known hydration

ΔA

energies of the cations. The overall thermodynamics of Cs^+/K^+ exchange reaction can be represented by the following equation

$$K^+ - X \quad + \quad Cs^+_{(aq)} \quad \rightarrow \quad Cs^+ - X \quad + \quad K^+_{(aq)} \qquad (1)$$

where X is the muscovite surface and ΔA is the Helmholtz free energy for the exchange reaction. Importantly, the muscovite surface (X) can be described as a sum of all different types of adsorption sites present. Our simulated muscovite surface is represented by 17% of **1a**, 33% of **1b**, and 50% of **1c** adsorption sites. The hydration energies for the cations (Cs^+/K^+) consistent with SPC water model were taken from the literature.[63]

Table 1 summarizes all the thermodynamic parameters necessary to evaluate the Cs^+/K^+ exchange reaction at the hydrated muscovite surface as a whole and at each individual adsorption site separately. It is important to keep in mind that all our simulations were performed using the *NVT* ensemble, hence the Helmholtz free energy of adsorption, ΔA, was estimated in our PMF calculations. The Gibbs free energy of adsorption, ΔG, is related to it by the equation $\Delta G = \Delta A + P\Delta V$. However, the PV term can be safely neglected here because at ambient pressure it is ~3-4 orders of magnitude smaller than the overall exchange energetics.[64] Thus, the cation exchange reactions (1) at different adsorption sites are largely controlled by the differences in the adsorption energy and the hydration energies of cations. Based on the calculated ΔG values of the site specific exchange reactions, it is evident that the adsorption site **1c** is the most favorable for Cs^+/K^+ ion exchange with ΔG = -54.4 kJ/mol, followed by the site **1b** (-49.0 kJ/mol), and the least favorable site is **1a** (-42.7 kJ/mol). However, the overall Cs^+/K^+ ion exchange energy at the muscovite surface weighted by the availability of various sites (site fractions) amounts to ΔG = -50.6 kJ/mol, while the intrinsic value of equilibrium cation exchange constant amounts to $\log K_{ex} = 8.8$ which is obtained from the equation

$$\Delta G_{ex} = -RT \ln K_{ex} = -2.303\ RT \log K_{ex}. \quad (2)$$

Table 1. Adsorption free energies (in kJ/mol) obtained from PMF calculations for K^+ and Cs^+ at three different sites on the hydrated muscovite basal surface and corresponding thermodynamic contribution to the Cs^+/K^+ cation exchange reaction (eq. 1).

Adsorption Site	K^+ - X	$Cs^+_{(aq)}$	Cs^+ - X	$K^+_{(aq)}$	ΔA	Site fraction	Energy fraction	log K_{ex}
1a	-41.8	-283.3	-29.3	-338.5	-42.7	0.167	-7.11	1.24
1b	-31.4		-25.1		-49.0	0.333	-16.32	2.83
1c	-25.1		-24.3		-54.4	0.500	-27.20	4.72
					Total	1.000	-50.63	8.79

At first glance, the energetics of the exchange reaction estimated from our simulations may seem quite different from the predictions based on the recent X-ray reflectivity measurements of Lee et al.[34] Indeed, the average K^+ adsorption free energy obtained from our simulations weighted by the availability of different site fractions (see Table 1), is equal to -30.0±1.0 kJ/mol, compared to -22.7±0.7 kJ/mol, and the corresponding values for Cs^+ adsorption are -25.4±1.0 kJ/mol and -21.2±0.8 kJ/mol, respectively. The larger energy difference between K^+ and Cs^+ may result, in part, from a much stronger preference for IS adsorption for K^+

in the simulations, while experimentally the IS/OS ratio is approximately 2/1.[34] This is due to the inability of the ClayFF model to reproduce accurately the ditrigonal distortion of the tetrahedral sheet[20,45,46] of phyllosilicates, leading to a somewhat larger size of the ditrigonal cavities of the siloxane surface by making them nearly hexagonal on average, thus leading to a somewhat stronger inner-sphere adsorption predicted by the models. However, recent molecular simulations of fixed muscovite substrate surface which fully retained the proper ditrigonal distortion of the tetrahedral rings[65] with the same ClayFF potential have yielded the near surface hydration and adsorption structure very similar to one observed with current and previous simulation studies[9,50-52] for a relaxed surface. Therefore, even if the adsorption energies reported here could be somewhat higher for a particular site than for a model where the ditrigonal shape of the ring is fixed, the energy differences between K^+ and Cs^+ ions and the site specific minima of the free energy profiles would follow the same characteristic pattern (**1a**>**1b**>**1c**).

In addition, the difference in the energetics of the exchange reaction between the predictions of the present model and the thermodynamic analysis of the X-ray reflectivity measurements[34] can be, in fact, the result of somewhat different approaches to the description of the exchange reaction in both cases. Experimentally, the free energy of adsorption of a metal cation was obtained as the sum of the adsorption free energies of inner sphere and outer sphere surface complex, and the ion exchange energies were calculated using the difference in the ΔG values between any metal cations. The ΔG and K_{ex} values estimated using such a definition of ion exchange reaction amounts to -4.6kJ/mol and 0.7, respectively, and are in reasonable agreement with the experimental energetics. However, it is important to have similar solution structure at larger distances during the ion exchange reaction as different cations exhibit variable hydration structures. Hence, in order to have a common reference for the exchange reaction, the hydration

energies of cations should also be considered for the calculation of the thermodynamic parameters. Therefore, the description of the ion exchange used for the estimation of the thermodynamic parameters listed in Table 1 appears to be a more general representation for any ion-exchange reaction.

Conclusions

By MD simulations with the ClayFF force field we were able to identify for both K^+ and Cs^+ ions three structurally different adsorption sites on the basal surface of muscovite mica. Irrespective of the cationic nature and the type of the adsorption site, K^+ and Cs^+ are preferably adsorbed at the center of ditrigonal (hexagonal) cavities as inner sphere surface complexes. Adsorption free energy profiles of both K^+ and Cs^+ ions were obtained for each of the three different adsorption sites by PMF calculations using the umbrella sampling procedure in which a harmonic distance constraint was applied between the cation and a surface site defined by the position of 6 oxygen atoms forming the ditrigonal (hexagonal) cavity of the site. In order to eliminate the lateral movements of the cations, a weak wall potential was additionally applied along the *x*-*y* directions, thus keeping the ions above a selected site at each distance *z* from the surface. The resulting quasi-one-dimensional adsorption free energy profiles $\Delta A(z)$ clearly indicate that for both K^+ and Cs^+ ions the site of type **1a** (Fig.1) gives rise to a noticeably stronger adsorption than the others. The thermodynamic analysis, which also takes into account the differences in the hydration energies of K^+ and Cs^+ ions is solution, shows that the Cs^+/K^+ exchange reactions can occur on the hydrated surface of muscovite in the following order of preferability: **1c** > **1b** > **1a**. Since the muscovite surface contains, on average, 1/6 of sites **1a**,

compared to 1/3 of sites **1b**, and 1/2 of sites **1c**, the total energy for the Cs^+/ K^+ equilibrium exchange reactions amounts to ΔG = -50.6 kJ/mol. The discrepancy between the exchange energies obtained in the current MD simulation study and the thermodynamic values obtained through the interpretation of recent X-ray reflectivity measurements[34] can most probably be attributed to the inability of the ClayFF models to accurately represent the ditrigonal distortions of the adsorbing tetrahedral rings of the siloxane surface and to the differences in the description of exchange reaction equilibria between the experimental conditions and the simplified conditions of our simulations.

Acknowledgements

This work was supported by the industrial chair "Storage and Management of Radioactive Waste" at the Ecole des Mines de Nantes, funded by ANDRA, Areva, and EDF. Generous allocations of supercomputing resources made available within the Distributed European Computing Initiative (projects DECI-07-NUWCLAY and DECI-11-COMPCLAY by the PRACE-2IP receiving funding from the European Community's FP7/ 2007-2013 under grant agreement RI-283493) and at the GENCI supercomputing facilities in France (projects x2012096921, x2013096921, and x2014096921) are also most gratefully acknowledged.

References

(1) Appelo, C. A. J.; Vinsot, A.; Mettler, S.; Wechner, S. Obtaining the Porewater Composition of a Clay Rock by Modeling the In- and Out-Diffusion of Anions and Cations from an In-Situ Experiment. *J. Contam. Hydrol.* **2008,** *101*, 67-76.

(2) Davis, J. A.; Kent, D. B. Surface Complexation Modeling in Aqueous Geochemistry. *Rev. Mineral.* **1990**, *23*, 177-260.

(3) Ochs, M.; Boonekamp, M.; Wanner, H.; Satp, H.; Yui, M. A Quantitative Model for Ion Diffusion in Compacted Bentonite. *Radiochim. Acta* **1998**, *82*, 437-444.

(4) Park, C.; Fenter, P.; Nagy, K. L.; Sturchio, N. C. Hydration and Distribution of Ions at the Mica-Water Interface. *Phys. Rev. Lett*. **2006**, *97*, 016101.

(5) Brown, G. E.; Henrich, V. E.; Casey, W. H.; Clark, D. L.; Eggleston, C.; Felmy, A.; Goodman, D. W.; Grätzel, M.; Maciel, G.; McCarthy, M. I.; Nealson, K. H.; Sverjensky, D. A.; Toney, M. F.; Zachara, J. M. Metal Oxide Surfaces and Their Interactions with Aqueous Solutions and Microbial Organisms. *Chem. Rev.* **1998,** *99*, 77-174.

(6) Henderson, M. A. The Interaction of Water with Solid Surfaces: Fundamental Aspects Revisited. *Surf. Sci. Reports* **2002,** *46*, 5-308.

(7) Kerisit, S.; Parker, S. C. Free Energy of Adsorption of Water and Metal Ions on the {1014} Calcite Surface. *J. Amer. Chem. Soc.* **2004**, *126*, 10152-10161.

(8) Kerisit, S.; Cooke, D. J.; Spagnoli, D.; Parker, S. C. Molecular Dynamics Simulations of the Interactions between Water and Inorganic Solids. *J. Mater. Chem.* **2005**, *15*, 1454-1462.

(9) Wang, J.; Kalinichev, A. G.; Kirkpatrick, R. J. Effects of Substrate Structure and Composition on the Structure, Dynamics, and Energetics of Water at Mineral Surfaces: A Molecular Dynamics Modeling Study. *Geochim. Cosmochim. Acta* **2006,** *70*, 562-582.

(10) Israelachvili, J. N. *Intermolecular and Surface Forces*; Academic press: New York, **1992**.

(11) Miranda, P. B.; Xu, L.; Shen, Y. R.; Salmeron, M. Icelike Water Monolayer Adsorbed on Mica at Room Temperature. *Phys. Rev. Lett.* **1998,** *81*, 5876-5879.

(12) Cantrell, W. C.; Ewing, G. E. Thin Film Water on Muscovite Mica. *J. Phys. Chem. B* **2001,** *105*, 5434-5439.

(13) Balmer, T. E.; Christenson, H. K.; Spencer, N. D.; Heuberger, M. The Effect of Surface Ions on Water Adsorption to Mica. *Langmuir* **2007**, *24*, 1566-1569.

(14) Lee, S. S.; Fenter, P.; Park, C.; Sturchio, N. C.; Nagy, K. L. Hydrated Cation Speciation at the Muscovite (001)-Water Interface. *Langmuir* **2010,** *26*, 16647-16651.

(15) Lee, S. S.; Park, C.; Fenter, P.; Sturchio, N. C.; Nagy, K. L. Competitive Adsorption of Strontium and Fulvic Acid at the Muscovite-Solution Interface Observed with Resonant Anomalous X-Ray Reflectivity. *Geochim. Cosmochim. Acta* **2010,** *74*, 1762-1776.

(16) Dzene, L.; Tertre, E.; Hubert, F.; Ferrage, E. Nature of the Sites Involved in the Process of Cesium Desorption from Vermiculite. *J. Colloid Interf. Sci*. **2015**, *455*, 254-260.

(17) Feibelman, P. J. K^+ Hydration in a Low-Energy Two-Dimensional Wetting Layer on the Basal Surface of Muscovite. *J. Chem. Phys.* **2013**, *139*, 074705-10.

(18) Spagnoli, D.; Cooke, D. J.; Kerisit, S.; Parker, S. C. Molecular Dynamics Simulations of the Interaction between the Surfaces of Polar Solids and Aqueous Solutions. *J. Mater. Chem.* **2006**, *16*, 1997-2006.

(19) Leng, Y.; Cummings, P. T. Hydration Structure of Water Confined between Mica Surfaces. *J. Chem. Phys.* **2006,** *124*, 074711-4.

(20) Meleshyn, A. Aqueous Solution Structure at the Cleaved Mica Surface: Influence of K^+, H_3O^+, and Cs^+ Adsorption.*J. Phys. Chem. C* **2008,** *112*, 20018-20026.

(21) Rotenberg, B. Water in Clay Nanopores. *MRS Bulletin* **2014**, *39*, 1074-1081.

(22) Holmboe, M.; Bourg, I. C. Molecular Dynamics Simulations of Water and Sodium Diffusion in Smectite Interlayer Nanopores as a Function of Pore Size and Temperature. *J. Phys. Chem. C* **2014**, *118*, 1001-1013.

(23) Ngouana Wakou, B. F.; Kalinichev, A. G. Structural Arrangements of Isomorphic Substitutions in Smectites: Molecular Simulation of the Swelling Properties, Interlayer Structure, and Dynamics of Hydrated Cs-Montmorillonite Revisited with New Clay Models. *J. Phys. Chem. C* **2014,** *118*, 12758-12773.

(24) Loganathan, N.; Yazaydin, A. O.; Bowers, G. M.; Kalinichev, A. G.; Kirkpatrick, R. J. Structure, Energetics, and Dynamics of Cs^+ and H_2O in Hectorite: Molecular Dynamics Simulations with an Unconstrained Substrate Surface. *J. Phys. Chem. C* **2016**, *120*, 10298-10310.

(25) Chen, Z.; Montavon, G.; Ribet, S.; Guo, Z.; Robinet, J. C.; David, K.; Tournassat, C.; Grambow, B.; Landesman, C. Key Factors to Understand In-Situ Behavior of Cs in Callovo-Oxfordian Clay-Rock (France). C*hemical Geology* **2014**, *387*, 47-58.

(26) Weng, L.; Van Riemsdijk, W. H.; Hiemstra, T. Effects of Fulvic and Humic Acids on Arsenate Adsorption to Geothite: Experiments and Modeling. *Env. Sci. Technol.* **2009**, *43*, 7198-7204.

(27) Bourg, I. C.; Sposito, G. Molecular Dynamics Simulations of the Electrical Double Layer on Smectite Surface Contacting Concentrated Mixed Electrolyte (NaCl-$CaCl_2$) Solutions. *J. Coll. Interf. Sci.* **2011**, *360*, 701-715.(28) Park, C.; Fenter, P. A.; Sturchio, N. C.; Nagy, K. L. Thermodynamics, Interfacial Structure, and pH Hysteresis of Rb^+ and Sr^{2+} Adsorption at the Muscovite (001)-Solution Interface. *Langmuir.* **2008**, *24*, 13993-14004.

(29) Schlegel, M. L.; Nagy, K. L.; Fenter, P.; Cheng, L.; Sturchio, N. C.; Jacobsen, S.D. Cation Sorption on the Muscovite (0 0 1) Surface in Chloride Solutions Using High-Resolution X-Ray Reflectivity. G*eochim. Cosmochim. Acta* **2006,** *70*, 3549-3565.

(30) Manceau, A.; Lanson, B.; Schlegel, M. L.; Eybert-Berard, L.; Hazemann, J. L.; Chateigner, D.; Lamble, G. M. Quantitative Zn Speciation in Smelter-Contaminated Soils by EXAFS Spectroscopy. *Am. J. Sci.* **2000**, *300*, 289-343.

(31) Sverjensky, D. A. Physical Surface-Complexation Models for Sorption at the Mineral-Water Interface. *Nature* **1993**, *364*, 776-780.

(32) Hiemstra, T.; Riemsdijk Van, W. H. On the Relationship between Charge Distribution, Surface Hydration, and the Structure of the Interface of Metal Hydroxides. *J. Coll. Interf. Sci.* **2006,** *301*, 1-18.

(33) Rahnemaie, R.; Hiemstra, T.; Riemsdijk Van, W. H. A New Surface Structural Approach to Ion Adsorption: Tracing the Location of Electrolyte Ions. *J. Coll. Interf. Sci.* **2006,** *293*, 312-321.

(34) Lee, S. S.; Park, C.; Fenter, P.; Sturchio, N. C.; Nagy, K. L. Changes in Adsorption Free Energy and Speciation During Competitive Adsorption between Monovalent Cations at the Muscovite (0 0 1)-Water Interface. *Geochim. Cosmochim. Acta* **2013,** *123*, 416-426.

(35) Kim, Y.; Kirkpatrick, R. J.; Cygan, R. T. Cs-133 NMR Study of Cesium on the Surfaces of Kaolinite and Illite. *Geochim. Cosmochim. Acta* **1996,** *60*, 4059-4074.

(36) Kim, Y.; Kirkpatrick, R. J. Na-23 and Cs-133 NMR Study of Cation Adsorption on Mineral Surfaces: Local Environments, Dynamics, and Effects of Mixed Cations. *Geochim. Cosmochim. Acta* **1997,** *61*, 5199-5208.

(37) Poinssot, C.; Baeyens, B.; Bradbury, M. H. Experimental and Modelling Studies of Caesium Sorption on Illite. *Geochim. Cosmochim. Acta* **1999**, *63*, 3217-3227.

(38) Zachara, J. M.; Smith, S. C.; Liu, C.; McKinley, J. P.; Serne, R. J.; Gassman, P. L. Sorption of Cs^+ to Micaceous Subsurface Sediments from the Hanford Site, USA. *Geochim. Cosmochim. Acta* **2002**, *66*, 193-211.

(39) de Koning, A.; Comans, R. N. J. Reversibility of Radiocaesium Sorption on Illite. *Geochim. Cosmochim. Acta* **2004**, *68*, 2815-2823.

(40) McKinley, J. P.; Zachara, J. M.; Heald, S. M.; Dohnalkova, A.; Newville, M. G.; Sutton, S. R. Microscale Distribution of Cesium Sorbed to Biotite and Muscovite. *Env. Sci. Technol.* **2004**, *38*, 1017-1023.

(41) Benedicto, A.; Missana, T.; Fernández, A. M. Interlayer Collapse Affects on Cesium Adsorption onto Illite. *Env. Sci. Technol.* **2014**, *48*, 4909-4915.

(42) Yasunari, T. J.; Stohl, A.; Hayano, R. S.; Burkhart, J. F.; Eckhardt, S.; Yasunari, T. Cesium-137 Deposition and Contamination of Japanese Soils due to the Fukushima Nuclear Accident. *Proc. Natl. Acad. Sci. U.S.A.* **2011**, *108*, 19530-19534.

(43) Okumura, M.; Nakamura, H.; Machida, M. Mechanism of Strong Affinity of Clay Minerals to Radioactive Cesium: First-Principles Calculation Study for Adsorption of Cesium at Frayed Edge Sites in Muscovite. *J. Phys. Soc. Jpn.* **2013**, *82*, 033802-5.

(44) Suehara, S.; Yamada, H. Cesium Stability in a Typical Mica Structure in Dry and Wet Environments from First-Principles. *Geochim. Cosmochim. Acta* **2013**, *109*, 62-73.

(45) Zaunbrecher, L. K.; Cygan, R. T.; Elliott, W. C. Molecular Models of Cesium and Rubidium Adsorption on Weathered Micaceous Minerals. *J. Phys. Chem. A* **2015**, *119*, 5691-5700.

(46) Lammers, L. N.; Bourg, I. C.; Okumura, M.; Kolluri, K.; Sposito, G.; Machida, M. Molecular Dynamics Simulations of Cesium Adsorption on Illite Nanoparticles. *Journal of Colloid and Interface Science* **2017**, *490*, 608-620.

(47) Kerisit, S.; Cooke, D. J.; Marmier, A.; Parker, S. C. Atomistic Simulation of Charged Iron Oxyhydroxide Surfaces in Contact with Aqueous Solution. *Chem. Commun.* **2005**, 3027-3029.

(48) Brigatti, M.F.; Guggenheim, S. Mica Crystal Chemistry and the Influence of Pressure, Temperature, and Solid Solution on Atomistic Models. *Rev. Mineral. Geochem*. **2002**, *46*, 1-97.

(49) Kuwahara, Y. Muscovite Surface Structure Imaged by Fluid Contact Mode AFM. *Phys. Chem. Minerals* **1999**, *26*, 198-205.

(50) Wang, J. W.; Kalinichev, A. G.; Kirkpatrick, R. J.; Cygan, R. T. Structure, Energetics, and Dynamics of Water Adsorbed on the Muscovite (001) Surface: A Molecular Dynamics Simulation. *J. Phys. Chem. B* **2005**, *109*, 15893-15905.

(51) Wang, J.; Kalinichev, A.G.; and Kirkpatrick, R.J. Asymmetric Hydrogen Bonding and Orientational Ordering of Water at Hydrophobic and Hydrophilic Surfaces: A Comparison of Water/Vapor, Water/Talc, and Water/Mica Interfaces. *J. Phys. Chem. C* **2009,** *113*, 11077-11085.

(52) Loganathan, N.; Kalinichev, A.G. On the Hydrogen Bonding Structure at the Aqueous Interface of Ammonium-Substituted Mica: A Molecular Dynamics Simulation. *Zeitschrift fur Naturforschung A* **2013**, *68*, 91-100.

(53) Teich-McGoldrick, S.L.; Greathouse, J.A.; Cygan, R.T. Molecular Dynamics Simulations of Uranyl Adsorption and Structure on the Basal Surface of Muscovite. *Molecular Simulation* **2014**, *40*, 610-617.

(54) Meleshyn, A. Potential of Mean Force for K^+ in Thin Water Films on Cleaved Mica. *Langmuir* **2010,** *26*, 13081-13085.

(55) Plimpton, S. Fast Parallel Algorithms for Short-Range Molecular Dynamics. *J. Comp. Phys.* **1995,** *117*, 1-19.

(56) Cygan, R. T.; Liang, J.-J.; Kalinichev, A. G. Molecular Models of Hydroxide, Oxyhydroxide, and Clay Phases and the Development of a General Force Field. J. *Phys. Chem. B* **2004,** *108*, 1255-1266.

(57) Phillips, C. J.; Braun, R.; Wang, W.; Gumbart, J.; Tajkhorshid, E.; Villa, E.; Chipot, C.; Skeel, R. D.; Kale, L.; Schulten, K. Scalable Molecular Dynamics with NAMD. *J. Comp. Chem.* **2005,** *26*, 1781-1802.

(58) Roux, B. The Calculation of the Potential of Mean Force Using Computer Simulations. *Comp. Phys. Comm.* **1995,** *91*, 275-282.

(59) Meleshyn, A. Potential of Mean Force for Ca^{2+} at the Cleaved Mica-Water Interface. *J. Phys. Chem. C* **2009,** *113*, 17604-17607.

(60) Kumar, S.; Bouzida, D.; Swendsen, R. H.; Kollman, E. A.; Rosenberg, J. M. The Weighted Histogram Analysis Method for Free-Energy Calculations on Biomolecules. I. The Method. *J. Comp. Chem.* **1992,** *13*, 1011-1021.

(61) Trzesniak, D.; Kunz, A.-P.E.; van Gunsteren, W.F. A Comparison of Methods to Compute the Potential of Mean Force. *ChemPhysChem* **2007**, *8*, 162-169.

(62) Lee, S. S.; Park, C.; Fenter, P.; Sturchio, N. C.; Nagy, K. L. Monovalent Ion Adsorption at the Muscovite (001) - Solution Interface: Relationships among Ion Coverage and Speciation, Interfacial Water Structure, and Substrate Relaxation. *Langmuir* **2012,** *28*, 8637-8650.

(63) Aqvist, J. Ion-Water Interaction Potentials Derived from Free Energy Perturbation Simulations. *J. Phys. Chem.* **1990,** *94*, 8021-8024.

(64) Rosso, K. M.; Rustad, J. R.; Bylaska, E. J. The Cs/K Exchange in Muscovite Interlayers: An Ab-Initio Treatment. *Clays and Clay Minerals* **2001**, *49*, 500-513.

(65) Malani, A.; Ayappa, K. G. Relxation and Jump Dynamics of Water at the Mica Interface. *J. Chem. Phys.* **2012**, *136*, 194701.

Table 1. Adsorption free energies (in kJ/mol) obtained from PMF calculations for K^+ and Cs^+ at three different sites on the hydrated muscovite basal surface and corresponding thermodynamic contribution to the Cs^+/K^+ cation exchange reaction (eq. 1).

Adsorption Site	K^+ - X	$Cs^+_{(aq)}$	Cs^+ - X	$K^+_{(aq)}$	ΔA	Site fraction	Energy fraction	log K_{ex}
1a	-41.8	-283.3	-29.3	-338.5	-42.7	0.167	-7.11	1.24
1b	-31.4		-25.1		-49.0	0.333	-16.32	2.83
1c	-25.1		-24.3		-54.4	0.500	-27.20	4.72
					Total	1.000	-50.63	8.79

Figure captions

Figure 1. Schematic representation of the hydrated basal muscovite surface illustrating 3 structurally different adsorption sites. Al – Pink; Si – yellow; O – red, H – white; K^+ – purple, Cs^+- cyan. (Only one tetrahedral sheet is shown for clarity).

Figure 2. A schematic view of the tetrahedral muscovite surface indicating the metal ions (K^+/Cs^+) probing a narrow cylindrical space normal to the muscovite surface above a specific adsorption site. The origin of the vector normal to the surface is defined by the center of mass of 6 surface bridging oxygen atoms of the ditrigonal ring forming the adsorption site.

Figure 3. Adsorption free energy profiles for K^+ ions as a function of distance for three different adsorption sites on the muscovite basal surface. The adsorption sites **1a**, **1b**, and **1c** are defined in Fig.1.

Figure 4. Adsorption free energy profiles for Cs^+ ions as a function of distance for three different adsorption sites on the muscovite basal surface. The adsorption sites **1a**, **1b**, and **1c** are defined in Fig.1.

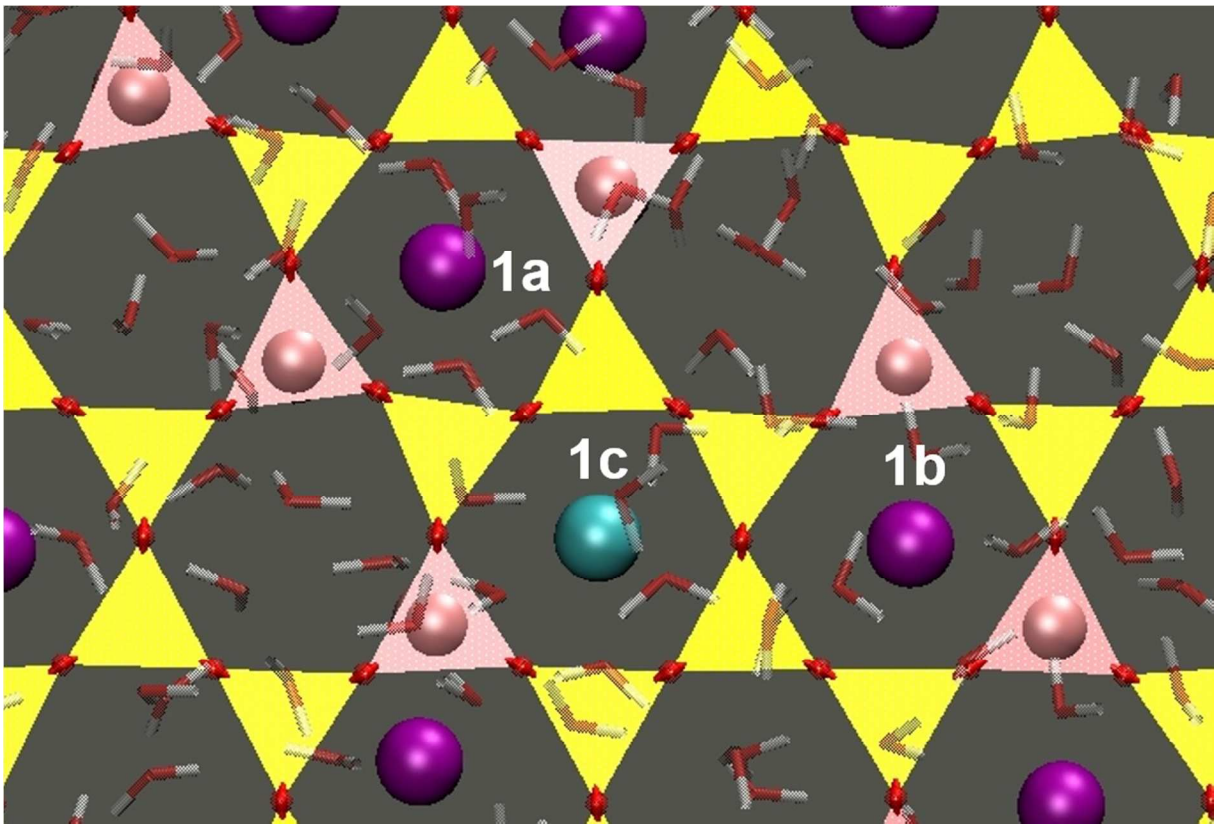

Fig. 1

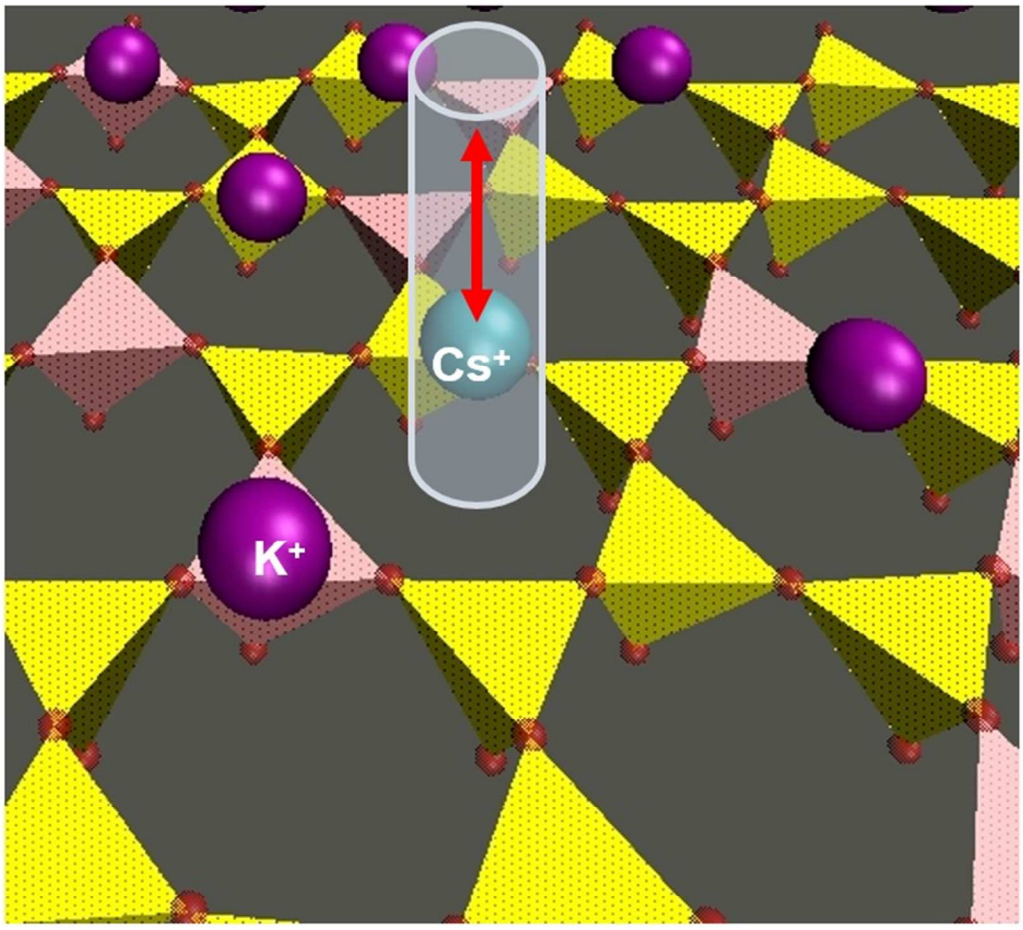

Fig.2

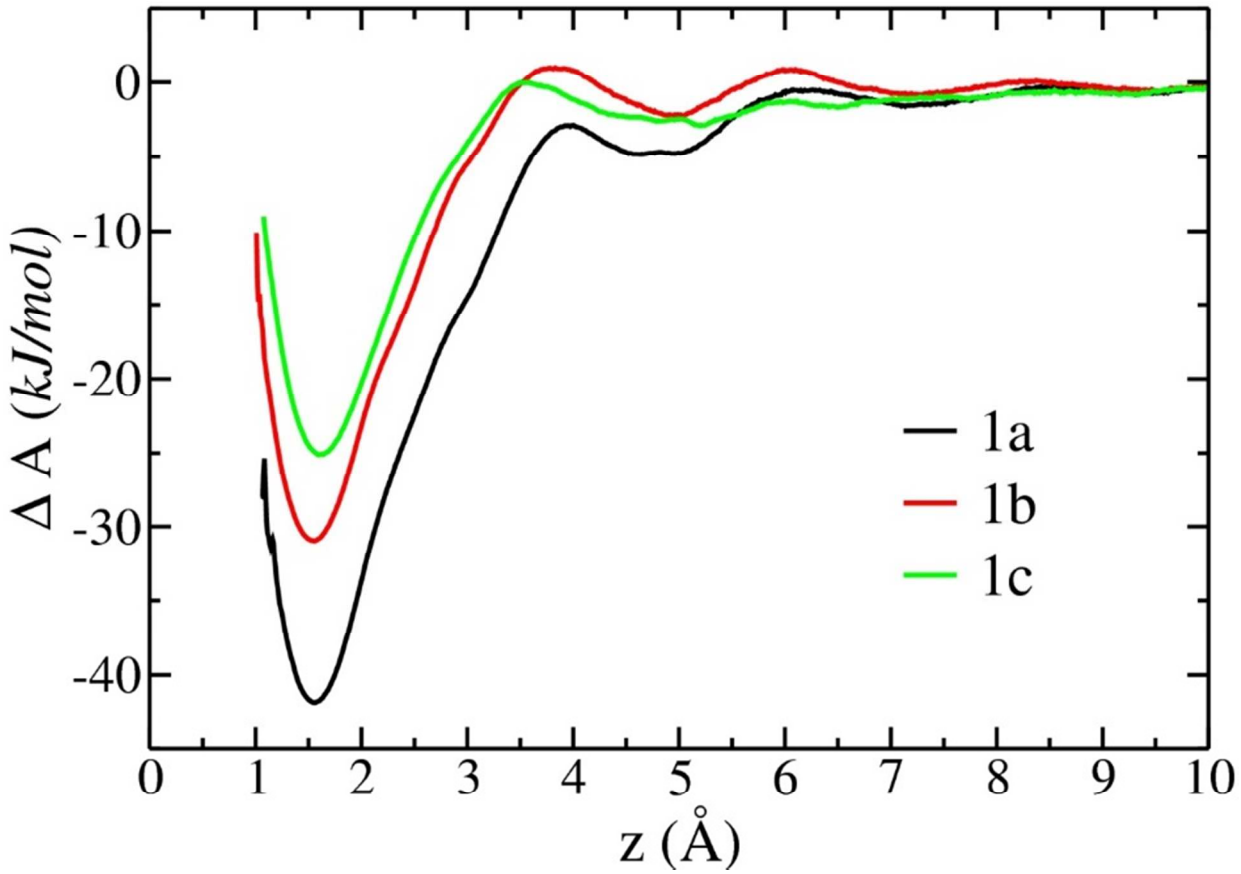

Fig. 3

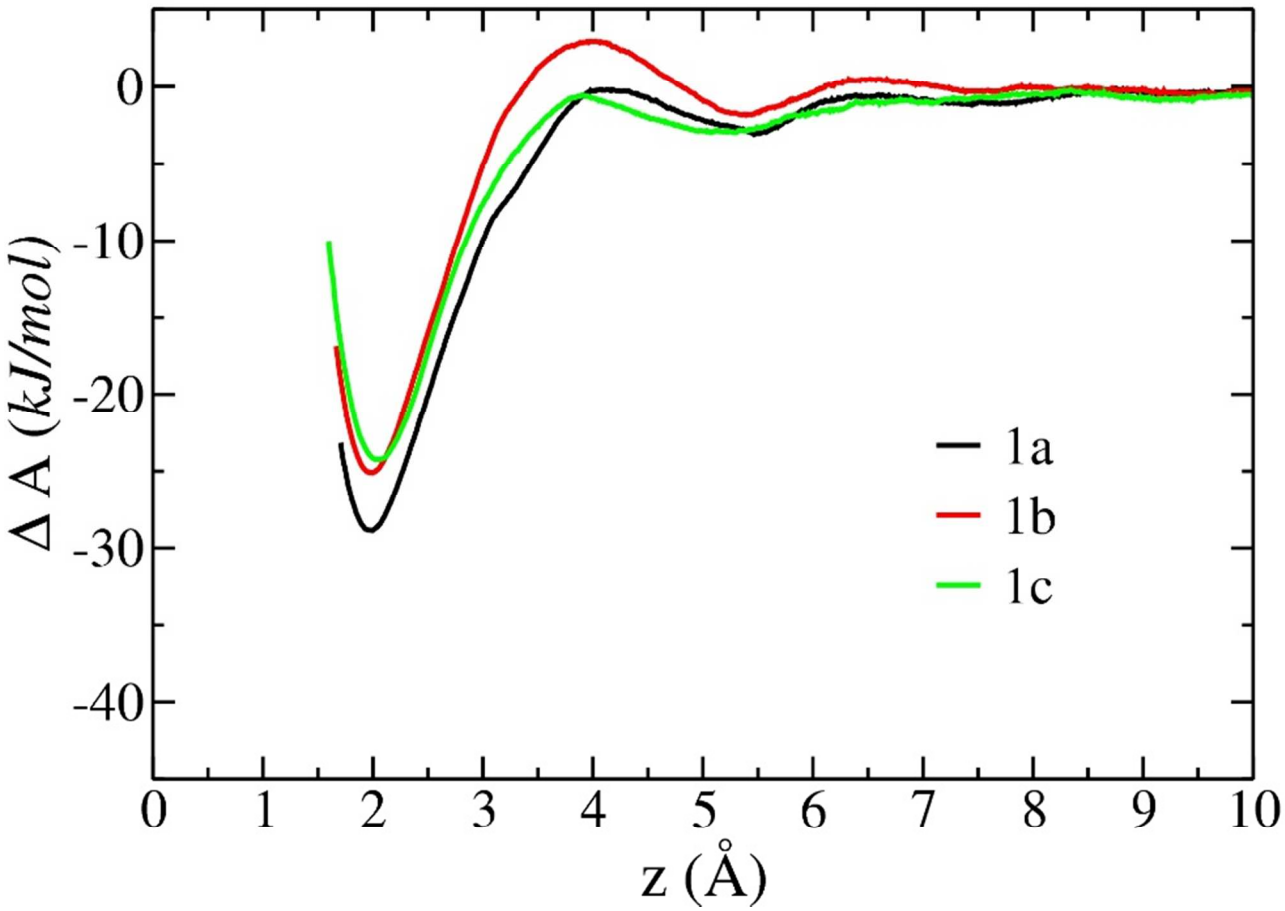

Fig. 4

TOC graphics